The Least–Squares Spectral Collocation Method for the Stokes and the Navier-Stokes equations: Conservation of mass and momentum

Thorsten Kattelans and Wilhelm Heinrichs

Abstract We present a new least-squares scheme that leads to a superior conservation of mass and momentum: The Least-Squares Spectral Collocation Method (LSSCM). From the literature it is known that the LSFEM has to be modified to obtain a mass conserving scheme. The LSSEM compensates the lack in conservation of mass by a superior conservation of momentum. The key for the superior conservation of mass and momentum of the LSSCM can be found in using only a few elements, the transfinite mapping of Gordon and Hall for discretization, the Clenshaw-Curtis quadrature rule for imposing the average pressure to be zero and using QR decomposition for solving the overdetermined algebraic systems to minimize the influence of round-off errors.

1 Introduction

For spectral methods it is well-known that if the velocity and the pressure are approximated by polynomials of the same degree eight spurious modes occur which lead to an instable system, see e.g. [1, 2, 4]. Least-squares discretizations avoid this problem and lead to symmetric positive definite systems, see e.g. [2]. For least-squares schemes it is a well-known problem that they perform poorly for internal flow problems (e.g. a cylinder that moves along a channel). The reason is that the equations must only be fulfilled in the least-squares sense. Least-squares spectral element methods compensate the lack in mass conservation by an superior conservation of momentum, see [16]. Here, we present a least-squares spectral collocation

Thorsten Kattelans
University of Duisburg-Essen, Engineering Mathematics, 45117 Essen, Germany, e-mail: thorsten.kattelans@uni-due.de

Wilhelm Heinrichs
University of Duisburg-Essen, Engineering Mathematics, 45117 Essen, Germany, e-mail: wilhelm.heinrichs@uni-due.de

scheme with an outstanding performance that leads to superior conservation of mass and momentum.

2 The Stokes and Navier-Stokes equations – Discretization

In order to apply least-squares the Stokes and Navier-Stokes problem is transformed into an equivalent first-order system of partial differential equations. This is accomplished by introducing the vorticity $\omega = \nabla \times \mathbf{u}$ as an auxiliary variable. Furthermore, the identity

$$\nabla \times \nabla \times \mathbf{u} = -\Delta \mathbf{u} + \nabla(\nabla \cdot \mathbf{u})$$

and the incompressibility constraint $\nabla \cdot \mathbf{u} = 0$ is used. Time integration is carried out by the standard BDF2 scheme for the viscous term combined with the second order Adams-Bashforth scheme for the convective term $\mathbf{C} := (\mathbf{u} \cdot \nabla)\mathbf{u}$. For a in-depth description, see, e.g. [9]. If now Δt denotes the step size in t and the index $n+1$ indicates that the functions are evaluated at the time step $t_{n+1} = (n+1)\Delta t$, $n = 0, 1, 2, \ldots$, the complete system at time step t_{n+1} can explicitly be written as

$$\begin{pmatrix} \frac{3}{2\Delta t} & 0 & \nu \frac{\partial}{\partial x_2} & \frac{\partial}{\partial x_1} \\ 0 & \frac{3}{2\Delta t} & -\nu \frac{\partial}{\partial x_1} & \frac{\partial}{\partial x_2} \\ \frac{\partial}{\partial x_2} & -\frac{\partial}{\partial x_1} & 1 & 0 \\ \frac{\partial}{\partial x_1} & \frac{\partial}{\partial x_2} & 0 & 0 \end{pmatrix} \begin{pmatrix} u_1^{n+1} \\ u_2^{n+1} \\ \omega^{n+1} \\ p^{n+1} \end{pmatrix} = \begin{pmatrix} \varphi_1^{n+1} \\ \varphi_2^{n+1} \\ 0 \\ 0 \end{pmatrix} \quad \text{in } \Omega_r, \tag{1}$$

where

$$\varphi^{n+1} = \mathbf{f}^{n+1} - 2\mathbf{C}^n + \mathbf{C}^{n-1} + \frac{2}{\Delta t}\mathbf{u}^n - \frac{1}{2\Delta t}\mathbf{u}^{n-1},$$

with $\varphi := [\varphi_1, \varphi_2]^T$. The big advantage of the explicit scheme is that the system of equations must only be solved once. During time integration we only have to compute matrix-vector multiplications which are very fast. By numerical experiments we found out that for a well balanced system it is recommended to scale the momentum equations by Δt, as in [8, 9, 12]. Then, for the least-squares scheme the incompressibility condition is well balanced against the momentum equations. In particular, we observed that without scaling the scheme becomes divergent for increasing Reynolds numbers since the diagonal entries $3/2\Delta t$ become large for decreasing step size, see, e.g. Figure 6 in [9]. For spatial discretization we use the Least-Squares

Spectral Collocation Method (LSSCM) where we use Clenshaw-Curtis quadrature rule for imposing the average pressure to be zero, see, e.g. [9, 12, 13]. The domain is decomposed into 12 quadrilaterals (some with curved boundaries, see Fig. 3 right) using the transfinite mapping of Gordon and Hall, where on each element Chebyshev Gauss-Lobatto (CGL) nodes are used for collocation. Along the interfaces we enforce pointwise continuity conditions for all unknown functions u_1, u_2, ω, p. Now, the discrete system of differential equations (on the corresponding element Ω_i denoted by A_i) together with the discrete boundary conditions (denoted by B), the discrete interface conditions (denoted by M_I) and the Clenshaw-Curtis quadrature (for the average pressure to be zero - denoted by M_P) are written into a matrix A and are compiled into an overdetermined system $Az = r$, where the matrix A is given by

$$A = \begin{pmatrix} A_1 & & \\ & \ddots & \\ & & A_{12} \\ & M_I & \\ & B & \\ & M_p & \end{pmatrix}. \tag{2}$$

3 The internal flow problem

In order to investigate the mass and momentum conservation of our LSSCM we use the same test case as in [3, 13, 15, 16]. The flow problem is defined by a cylinder of diameter d which moves at a speed of one along the centerline of a channel of width $h = 1.5$, see Fig. 1. The domain of the channel is defined as a rectangle and

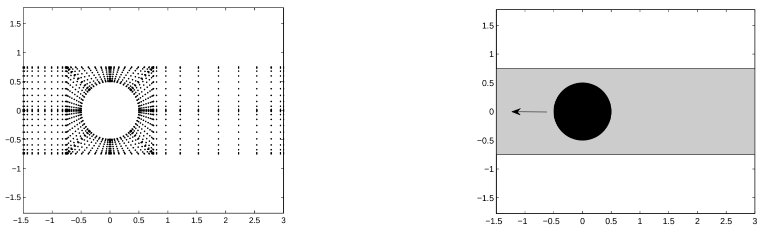

Fig. 1 The internal flow problem on $\Omega_{0.5}$: Discretization (left) and problem set-up (right)

the center of the cylinder is located at the origin, i.e. we solve the partial differential equations on the domain

$$\Omega_r := \Omega_c \backslash K_r,$$

where $\Omega_c := [-1.5,3] \times [-0.75,0.75]$ and $K_r := \left\{(x,y) \in \mathbb{R}^2 : x^2+y^2 < r^2\right\}$. The boundary conditions of the velocity are given by

$$\mathbf{u}_{|\partial\Omega_r} := \begin{cases} [1,0]^T \text{ on } \partial\Omega_c \\ [0,0]^T \text{ on } \partial K_r \end{cases} .$$

4 Numerical simulation

For the numerical experiments we consider the steady Stokes equations (with $\nu = 1$) and summarize results in the literature. The new numerical results are presented for the incompressible Navier-Stokes equations. We compare the performance of our scheme for different viscosities concerning conservation of mass and momentum.

4.1 Stokes equations

In [13] we have seen, that the LSSCM leads to an outstanding performance concerning conservation of mass and momentum. In Table 1 we show the results and compare them with other values, available in the literature (with $\nu = 1$). The presented values mean that mass and momentum, respectively, are conserved up to this value. The reason that the LSSCM leads to such outstanding results can be found in using

Table 1 Mass and Momentum conservation of different least-squares schemes for the steady Stokes equations on $\Omega_{0.5}$

Method	Mass conservation	Momentum conservation	Velocity profile	Reference
standard LSFEM	—	—	invalid	[3]
restricted LSFEM	10^{-4}	n/a	ok	[3]
standard LSSEM	10^{-1}	10^{-4}	ok	[16]
standard LSSCM	10^{-8}	10^{-7}	ok	[13]

only a few elements, using QR decomposition instead forming normal equations for solving the overdetermined algebraic systems, using Clenshaw-Curtis quadrature for imposing the average pressure to be zero and using the transfinite mapping of Gordon and Hall for the discretization, see [13].

4.2 Navier-Stokes equations

For the Navier-Stokes equations we define

$$\mathscr{M}_\psi := \int_{\gamma_1} \psi\, ds - \int_{\gamma_2} \psi\, ds, \tag{3}$$

where

$$\begin{aligned}\gamma_1 &:= \{(-1.5, y) : -1.5 \le y \le 1.5\},\\ \gamma_2 &:= \{(0, y) : -1.5 \le y \le -0.125\} \cup \{(0, y) : 0.125 \le y \le 1.5\}.\end{aligned}$$

The line integrals in (3) are evaluated using Clenshaw-Curtis quadrature. To avoid the influence of the quadrature rule to the value of $\mathscr{M}_\psi$, the integrals are approximated on refined lines. To see the influence of the viscosity to the mass and momentum conservation, we show the results for different ν in one plot. For $\nu = 1$ we use $\Delta t = 1/10$, for $\nu = 400^{-1}$ we use $\Delta t = 1/700$ and for $\nu = 600^{-1}$ we use $\Delta t = 1/1100$. In Fig. 2 we present the loss of mass along the cross-section γ_2 during time integration for different viscosities.

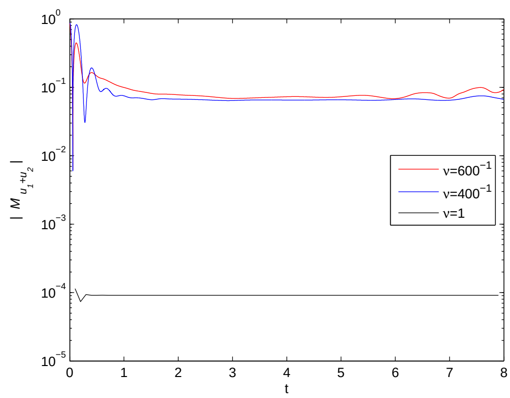

Fig. 2 Navier-Stokes flow past the cylinder on $\Omega_{0.125}$: Loss of mass along the cross-section for $\nu \in \{1, \frac{1}{400}, \frac{1}{600}\}$ with $\psi = u_1 + u_2$ during time integration

From Fig. 2 we observe the well-known performance that the loss of mass increases for decreasing viscosities, i.e. for increasing Reynolds numbers. For $\nu = \frac{1}{400}$ and $\nu = \frac{1}{600}$ there are no big differences in the results since for these viscosities we reach similar Reynolds numbers. Here, we see clearly that the "Von Karman Effect" occurs earlier for the larger Reynolds number. In Fig. 3 and 4 we show the conservation of the different velocity components along γ_2. As we observe from the plot in Fig. 3 our scheme leads to the same values during time integration for this stationary problem if the initial conditions are overcome. Fig. 4 shows the well-known oscillations for $\psi = u_2$. Thus, our scheme leads to the well-known performance for such a channel flow problem.

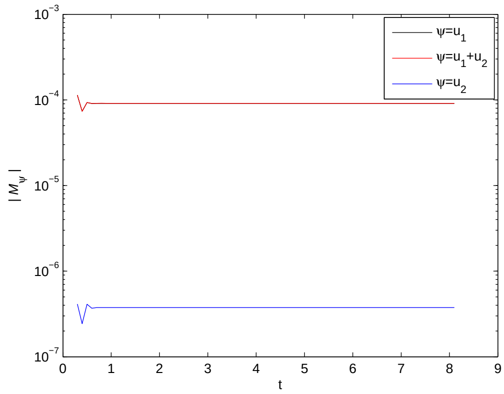

Fig. 3 Navier-Stokes flow past the cylinder on $\Omega_{0.125}$: Loss of mass along γ_2 for $\nu = 1$, where $\psi = u_1$, $\psi = u_2$ and $\psi = u_1 + u_2$

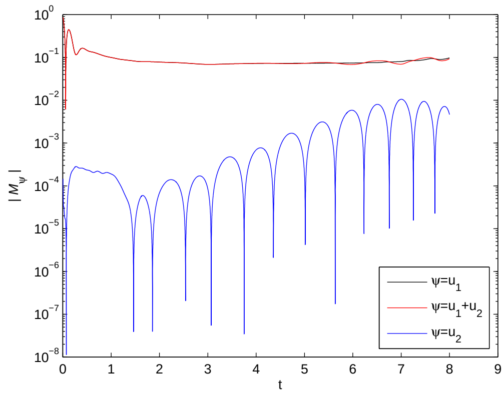

Fig. 4 Navier-Stokes flow past the cylinder on $\Omega_{0.125}$: Loss of mass along γ_2 for $\nu = \frac{1}{600}$, where $\psi = u_1$, $\psi = u_2$ and $\psi = u_1 + u_2$

In Fig. 5 we show the divergence of the velocity field for the different viscosities in the whole domain $\Omega_{0.125}$ during time integration. Since we collocate on CGL nodes we use Chebyshev-Gauss (CG) nodes to evaluate $\|\nabla \cdot \mathbf{u}\|_{L^2}$ obtaining the real conservation and not the least-squares error. Again, we observe the well-known performance for the different viscosities. Comparing the divergence for $\nu = \frac{1}{400}$ and $\nu = \frac{1}{600}$ we see the earlier occurrence of the “Von Karman Effect” for the smaller viscosity, again. This is represented in the plot by the oscillation of the divergence.

Momentum conservation for the different viscosities is presented in Fig. 6. Again, we use CG nodes to evaluate the error of the (on CGL nodes) computed solutions. To compute the solutions we have to scale the momentum equations by Δt to obtain a stable scheme, where all involved equations are well balanced. Obtaining the real conservation of momentum we use this computed solutions and evaluated this in the unscaled system of partial differential equations. Thus, the results in Fig. 6 are not as good as the results in Fig. 5. Furthermore, the conservation of momentum is influenced by the velocity, vorticity and by the pressure, whereas

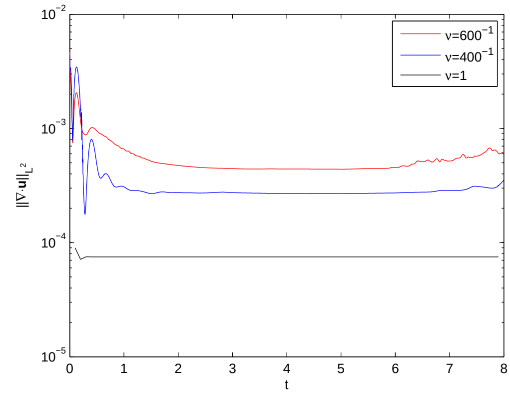

Fig. 5 Navier-Stokes flow past the cylinder on $\Omega_{0.125}$: $||\nabla \cdot \mathbf{u}||_{L^2}$ in the whole domain during time integration for $\nu \in \{1, \frac{1}{400}, \frac{1}{600}\}$

the conservation of mass is only influenced by the velocity.
The well-known performance of our scheme is observed, again, from both of the figures. Furthermore, we see that the oscillating starts earlier for the larger Reynolds number, as expected.

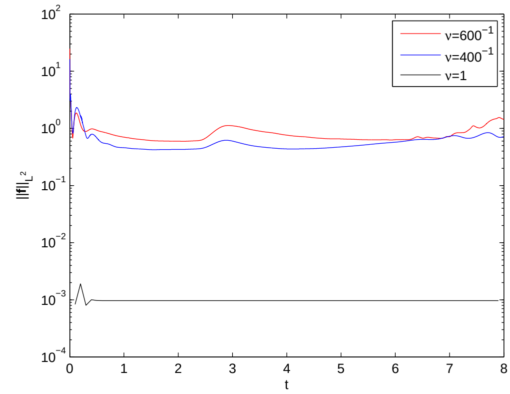

Fig. 6 Navier-Stokes flow past the cylinder on $\Omega_{0.125}$: $||\mathbf{f}||_{L^2}$ in the whole domain during time integration for $\nu \in \{1, \frac{1}{400}, \frac{1}{600}\}$

5 Conclusion

We studied the conservation of mass and momentum of the Least-Squares Spectral Collocation Method (LSSCM) for the incompressible Navier-Stokes equations using an internal flow problem. For least-squares schemes for such problems in general it is known that they have problems with mass conservation. For the Stokes equations the LSFEM does not conserve mass and must be modified by a restriction, see, e.g. [3]. Using the LSSEM for the Stokes equations leads to good results, since the LSSEM compensates the lack in conservation of mass by an superior conservation of momentum, see, e.g. [16]. As shown in the present paper, the LSSCM leads to superior conservation of mass and momentum for the Stokes and the Navier-Stokes equations. Thus, the LSSCM is an interesting alternative to other least-squares schemes such as the LSSEM or the LSFEM.

References

1. Bernardi, C., Canuto, C., Maday, Y.: Generalized inf–sup condition for Chebyshev approximations to the Navier–Stokes equations. C.R. Acad. Sci. Paris **303**, 971–974 (1986)
2. Canuto, C., Hussaini, M. Y., Quarteroni, A., Zang, T.A.: Spectral Methods — Evolution to Complex Geometries and Applications to Fluid Dynamics. Springer, Berlin Heidelberg (2007)
3. Chang, C.L., Nelson, J.J.: Least–squares finite element method for the Stokes problem with zero residual of mass conservation. SIAM J. Numer. Anal. **34**, 480–489 (1997)
4. Deville, M. O., Fischer, P. F., Mund, E.H.: High–Order Methods for Incompressible Fluid Flow. Cambridge University Press (2002)
5. Gordon, W. J., Hall, C. A.: Construction of curvilinear co–ordinate systems and their applications to mesh generation. Int. J. Numer. Meth. Eng. **7**, 461–477 (1973)
6. Gordon, W. J., Hall, C. A.: Transfinite element methods: blending–function interpolation over arbitrary curved element domains. Numer. Math. **21**, 109–129 (1973)
7. Heinrichs, W.: Spectral collocation schemes on the unit disc. J. Comput. Phys. **199**, 66–86 (2004)
8. Heinrichs, W.: Least-Squares Spectral Collocation for the Navier-Stokes Equations. J. Sci. Comput. **21**, 81–90 (2004)
9. Heinrichs, W., Kattelans, T.: A direct solver for the least–squares spectral collocation system on rectangular elements for the incompressible Navier–Stokes equations. J. Comput. Phys. **227**, 4776–4796 (2008)
10. Jiang, B.: The Least–Squares Finite Element Method: Theory and Applications in Computational Fluid Dynamics and Electromagnetics. Springer, Berlin (1998)
11. Jiang, B.: On the least–squares method. Methods Appl. Mech. Eng. **152**, 239–257 (1998)
12. Kattelans, T., Heinrichs, W.: A least–squares spectral collocation scheme with improved stability for the Stokes and the Navier–Stokes equations. In: Simos, T. E., Psihoyios, G., Tsitouras, Ch. (eds.) Numerical Analysis and Applied Mathematics, pp. 307–310. Springer, Berlin (2008)
13. Kattelans, T., Heinrichs, W.: Conservation of mass and momentum of the least–squares spectral collocation scheme for the Stokes problem. J. Comput. Phys. **228**, 4649–4664 (2009)
14. Peyret, R.: Spectral Methods for Incompressible Viscous Flow. Springer, New York (2002)
15. Proot, M. M. J.: The Least-Squares Spectral Element Method. Theory, Implementation and Application to Incompressible Flows. Ph.D thesis, Delft University of Technology (2003)
16. Proot, M. M. J., Gerritsma, M. I.: Mass– and Momentum Conservation of the Least–Squares Spectral Element Method for the Stokes Problem. J. Sci. Comput. **27**, 389–401 (2006)